

Swift GRBs: The early afterglow spectral energy distribution^(*)

G. TAGLIAFERRI⁽¹⁾, D. MALESANI⁽²⁾⁽³⁾, S. D. VERGANI⁽⁴⁾⁽⁵⁾, S. CAMPANA⁽¹⁾,
G. CHINCARINI⁽¹⁾⁽⁶⁾, S. COVINO⁽¹⁾, C. GUIDORZI⁽¹⁾⁽⁶⁾, A. MORETTI⁽¹⁾,
P. ROMANO⁽¹⁾⁽⁶⁾, L. A. ANTONELLI⁽⁷⁾, M. CAPALBI⁽⁸⁾, M. L. CONCIATORE⁽⁸⁾,
G. CUSUMANO⁽⁹⁾, P. GIOMMI⁽⁸⁾, V. LA PAROLA⁽⁹⁾, V. MANGANO⁽⁹⁾, T. MINEO⁽⁹⁾,
M. PERRI⁽⁸⁾ and E. TROJA⁽⁹⁾

⁽¹⁾ *INAF, Osservatorio Astronomico di Brera - Via E. Bianchi 46, I-23807 Merate (Lc), Italy*

⁽²⁾ *SISSA-ISAS - Via Beirut 2-4, I-34014 Trieste, Italy*

⁽³⁾ *Dark Cosmology Centre, Niels Bohr Institute - J. Maries vej 30, DK-2100 København Denmark*

⁽⁴⁾ *Dunsink Observatory - Castleknock, Dublin 15, Ireland*

⁽⁵⁾ *School of Physical Sciences and NCPST, Dublin City University - Dublin 9, Ireland*

⁽⁶⁾ *Università degli Studi di Milano-Bicocca - P.zza delle Scienze 3, I-20126 Milano, Italy*

⁽⁷⁾ *INAF, Osservatorio Astronomico di Roma - Via Frascati 33, I-00040 Monteporzio, Italy*

⁽⁸⁾ *ASI Science Data Center - Via G. Galilei, I-00044 Frascati (Roma), Italy*

⁽⁹⁾ *INAF, IASF Palermo - Via U. La Malfa 153, I-90146 Palermo, Italy*

(ricevuto il 6 Marzo 2007; pubblicato online il 13 Giugno 2007)

Summary. — We present the first results of a program to systematically study the optical-to-X-ray Spectral Energy Distribution (SED) of *Swift* GRB afterglows with known redshift. The goal is to study the properties of the GRB explosion and of the intervening absorbing material. In this report we present the preliminary analysis on 23 afterglows. Thanks to *Swift*, we could build the SED at early times after the GRB (minutes to hours). We derived the hydrogen column densities and the spectral slopes from the X-ray spectrum. We then constrained the visual extinction by requiring that the combined optical/X-ray SED is due to synchrotron, namely either a single power law or a broken power law with a slope change by 0.5. We confirm a low dust-to-metal ratio, smaller than in the SMC, even from the analysis of data taken significantly earlier than previously possible. Our analysis does not support the existence of “grey” dust. We also find that the synchrotron spectrum works remarkably well to explain afterglow SEDs. We clearly see, however, that during the X-ray steep decay phases and the flares, the X-ray radiation cannot be due only to afterglow emission.

PACS 98.70.Rz – γ -ray sources; γ -ray bursts.

^(*) Paper presented at the Workshop on “Swift and GRBs: Unveiling the Relativistic Universe”, Venice, June 5-9, 2006.

1. – Introduction

All evidences are that long-duration Gamma-Ray Bursts (GRBs) are associated with the death of massive stars that explode as type-Ic supernovae. GRBs seem to be associated with the very energetic subclass of hypernovae, whose features have been unambiguously identified in at least four cases: GRB 980425, GRB 030329, GRB 031203 and GRB 060218 [1-6]. Therefore, long-duration GRBs likely occur in the same regions where their massive progenitors were born and rapidly evolve. If these regions are similar to the giant molecular clouds in our Galaxy, then long-duration GRBs explode inside dense, dusty environments. The huge energy emitted in the gamma-ray band during the prompt emission phase is almost unaffected by absorption, allowing the detection of GRBs up to very high redshifts (*e.g.* [7-9]). On the other hand, emission at optical X-ray wavelengths is significantly affected by matter along the line of sight (hydrogen, gas, and dust). By studying afterglow spectra, we can then infer the properties of the intervening matter, both in the proximity of the explosion and along the line of sight. Furthermore, studying the afterglow behaviour allows the investigation of the explosion physics. In fact both issues must be handled together, since absorption modifies the observed spectrum, thus affecting the comparison with models; on the other hand, the properties of the intervening matter can be probed effectively only with an estimate of the intrinsic spectrum.

The standard model predicts that the afterglow radiation is produced by synchrotron emission during the slowing down of a relativistic fireball which impacts against the surrounding material. This model has proven successful in explaining the overall properties of afterglows, predicting, as observed, power law shapes for both the light curves and the spectra [10]. Well-defined relations are set between the decay and spectral power law indices (the so-called closure relations), which have been tested observationally. Despite an overall agreement, the wealth of accumulated data has highlighted a complex situation, which has led many authors to introduce several new ingredients, among which energy injection, radiative losses, non-standard density profiles, angular structure, and varying microphysical parameters [11-13]. The introduction of these effects has been more or less capable to explain the new data, but has partly reduced the predictive power of models, and the theoretical picture is not yet fully established. On the other hand, most of these solutions are still based on the idea that the observed spectrum is due to synchrotron emission. Independent of the details, the broad-band spectral shape can thus be computed from robust first principles, and from optical through X-ray frequencies it has the shape of a broken power law. With typical parameters, the break frequency is interpreted as the cooling break. In this case, a robust prediction is that the low- and high-energy spectral indices β_1 and β_2 differ by exactly 0.5 ($F_\nu \propto \nu^{-\beta}$): $\beta_1 = (p-1)/2$ and $\beta_2 = p/2$, where $p \approx 2$ is the index of the electron energy distribution (*e.g.* [14]). The position of the break frequency can however vary significantly from burst to burst (and it evolves with time for each case).

ISM intervening material affects the observed GRB spectrum by selectively extinguishing the radiation. At X-ray frequencies, the absorption is due to metals (either in the gas or dust phase), which affect mostly the low-energy range (below ≈ 0.5 keV). At optical and ultraviolet wavelengths, the spectral shape is modified by dust. GRBs are very interesting sources for probing the interstellar medium in the Universe, for a number of reasons. First, they are very bright. Second, the intrinsic spectral shape is simple enough to allow a reliable determination of the absorption amount. They are also observable across a wide range of wavelengths allowing to probe complementary aspects of the ISM. A lot of work has been already carried out in this respect. Optical and X-ray spectra have shown that GRBs explode in dense environments, as it is expected

for sources located inside star-forming regions [15, 16]. The metallicity is generally low ($Z \sim 0.1Z_{\odot}$), as inferred from both absorption-line measurements [15, 17] and from integrated spectra of a few host galaxies [18, 19]. Furthermore, there is very little dust content (*e.g.* [20]), actually much less than expected even for such low metallicities [21].

To gather information on the physical properties of the afterglows and of the intervening absorbing material, we started a program to study the optical-to-X-ray spectral energy distribution (SED) of *Swift* GRBs with known redshift. With respect to previous works (see, *e.g.*, [22-25]), thanks to *Swift* we can now extend the study to much earlier epochs. We can therefore check if there is evolution in the properties of both the absorbing material and the afterglow emission.

2. – Absorption and SEDs

The dust content (parametrized by the optical extinction A_V) is usually determined by fitting the photometric spectrum with an absorbed power law. This procedure, however, is strongly sensitive to the adopted extinction law, which is poorly known for the high-redshift ISM surrounding GRB sources. The most remarkable feature of GRB dust is the lack of the 2150 Å bump ubiquitously observed along Milky Way sight lines, leading to a preference for an SMC-like extinction curve [22, 24]. This makes it even more difficult to estimate the amount of total absorption, since a featureless extinction curve can be hardly disentangled from a power law shape unless good-quality photometry is available.

We present here a complementary approach to determine the dust content along GRB sight lines, by modelling the combined optical and X-ray spectral energy distribution, under the basic assumption that it is described by a synchrotron spectrum. This task has been already performed by several authors using a number of afterglows in the pre-*Swift* era [22, 25]. Our aim is to carry on a full study of the *Swift* sample. This kind of analysis is potentially suffering from a selection bias, namely the requirement that the burst is detected at optical wavelengths. Dusty afterglows more frequently escape detection and, even if detected, they may lack detailed photometric and spectroscopic studies. *Swift* provides rapid and precise GRB triggers, allowing a much more efficient follow up, therefore effectively reducing this bias.

To build the optical-to-X-ray SED we interpolated at a common time (from a few minutes to hours after the GRB) optical and X-ray data. We took optical data from the literature (including the GCNs) and from our own VLT and TNG MISTICI data, after rejecting clearly discrepant or miscalibrated points. We decided not to extract SEDs during complex phases of the light curves, rather we chose appropriate epochs with the best available spectral coverage. To avoid degeneracy in the modeling of the dust properties, we also selected bursts with measured (spectroscopic) redshift.

The XRT data were analysed following standard procedures. We concentrated mainly on the X-ray data obtained during the first two *Swift* orbits after the burst, from ~ 100 s up to 2-3 h (although we looked at the full light curve and in some cases extracted also SEDs at later times). In these early phases, the X-ray light curves are characterised by a complex behaviour, following the usual steep-flat-steep sequence, often with superimposed flares (*e.g.* [26-28]; figs. 2, 3). When relevant, we accumulated different spectra for each of these phases. Then we fitted them assuming an absorbed power law model, considering the absorption both in the Milky Way and local to the GRB. This model always provided a good fit to our data.

To measure the optical extinction, we started by computing the X-ray spectral slope β_X through fits to the XRT spectra. We then computed the dust extinction by requiring

GRB	z	GRB	z	GRB	z
050126	1.29	050814	5.3	060210	3.91
050223	0.59	050820A	2.612	060218	0.03
050315	1.949	050826	0.297	060223A	4.41
050318	1.44	050824	0.83	060418	1.49
050319	3.24	050904	6.295	060502	1.51
050401	2.90	050908	3.344	060505	0.089
050408	1.236	050922C	2.199	060510B	4.9
050416A	0.653	051016B	0.936	060512	0.443
050505	4.27	051109A	2.346	060522	5.11
050525A	0.606	051109B	0.08	050526	3.21
050603	2.821	051111	1.55	060604	2.68
050730	3.967	060115	3.53	060605	3.7
050802	1.71	060124	2.297	060607A	3.082
050803	0.422	060206	4.048	060614	0.125

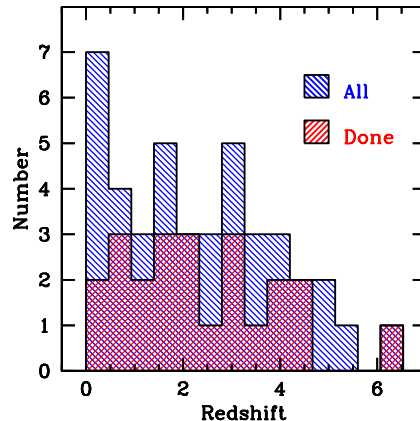


Fig. 1. – Left: list of GRBs included in our sample; bursts in boldface font were analyzed in this preliminary work. Right: redshift distribution of the full and analyzed samples. The average redshift is comparable for the two distributions ($\langle z \rangle = 2.32$ and 2.34).

either that a) the optical and X-ray spectra lie on the same power law component ($\beta_{\text{opt}} = \beta_{\text{X}}$) or that b) the cooling frequency lies between the two bands, so that $\beta_{\text{opt}} = \beta_{\text{X}} - 0.5$. To choose among the two possibilities, we compared the relative normalizations of the optical and X-ray components: for example, in case a) it is also necessary that the optical flux matches the extrapolation of the X-ray spectrum. If both solutions do not work, this would imply either a more complex spectral shape or a peculiar extinction curve. In our sample, however, all cases but one fit the simplest model. Note that we did *not* fit the optical data to find the extinction, but imposed a correction to match the constraint from the X-ray slope. To model the extinction, we adopted both the SMC extinction curve [29] and the “attenuation curve” derived for starburst (SB) galaxies by [30]. Our method has the advantage of being less sensitive to small errors in the photometric data, since the overall extinction is constrained by the knowledge of the intrinsic slope.

3. – Results

The sample we have selected contains 42 *Swift* long-duration GRBs with spectroscopic redshift up to 2006 June. In this report we present our preliminary results on 23 of them. Figure 1 shows the redshift distribution of the full sample and of the analyzed one.

3.1. The intervening matter. – As an example, we show in figs. 2 and 3 the light curves and SEDs of GRB 050319 and XRF 050416A. In the X-ray band, GRB 050319 shows the canonical steep-flat-steep behaviour (fig. 2, left panel; [31]). At optical wavelengths the behaviour is described by a single power law. Focussing on the late SED (taken during the flat X-ray phase), the presence of dust is evidenced by the steep observed spectral index $\beta_{\text{opt}} = 2.8$ (dashed line, right panel). However, after setting $A_V = 0.25$ mag, the optical spectrum is much less steep and lie on the same power law of the X-ray spectrum. This interpretation, *i.e.* that the two components are due to the same power law, is confirmed by the consistency of the temporal decay slopes in the two bands (for $t < 30$ ks). Figure 3 shows the light curve and SED of XRF 050416A. Again, focussing

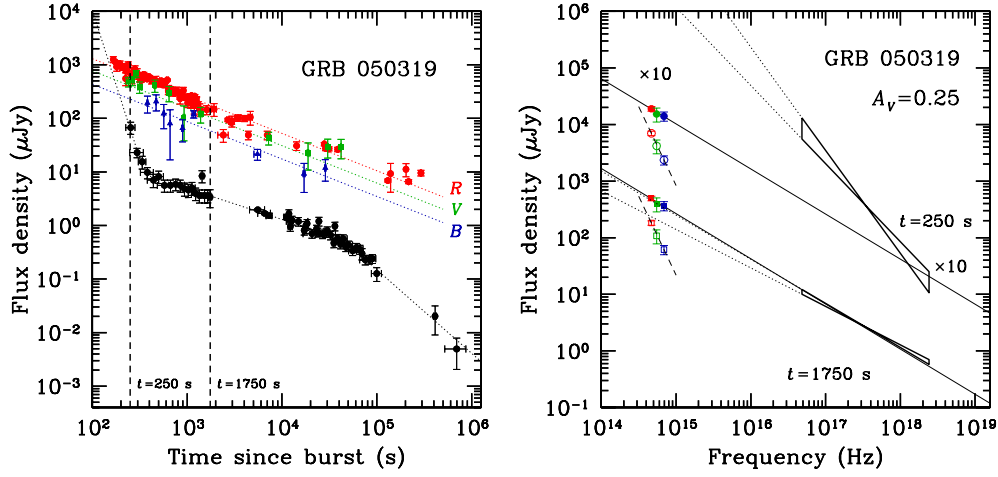


Fig. 2. – Left: optical and X-ray light curves of GRB 050319 (data from [31-34]). The vertical dashed lines mark the epochs at which we computed the SED (observer frame). Right: SED of GRB 050319 at the two epochs marked in the left panel. Empty symbols are not corrected for the host extinction, while filled symbols are. The solid and dotted lines indicate the extrapolation of the optical and X-ray spectra, respectively.

on the later SED, the dust effect is evident, but the cooling frequency was in this case lying between the optical and X-ray bands, at $\nu \sim 2 \times 10^{16}$ Hz.

Figure 4 (left panel) shows the distribution of the measured A_V with the two adopted extinction curves. The average values are $\langle A_V \rangle = 0.22 \pm 0.26$ and 0.39 ± 0.33 mag for the SMC and SB (Calzetti) curves, respectively. The SB extinction curve is flatter, so that

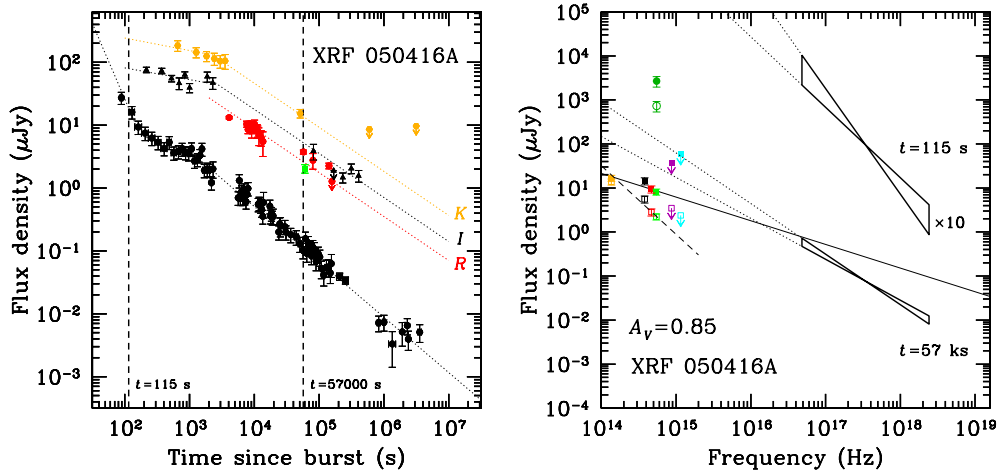


Fig. 3. – Left: optical and X-ray light curves of XRF 050416A (data from [35-37]). The style conventions are the same as in fig. 2.

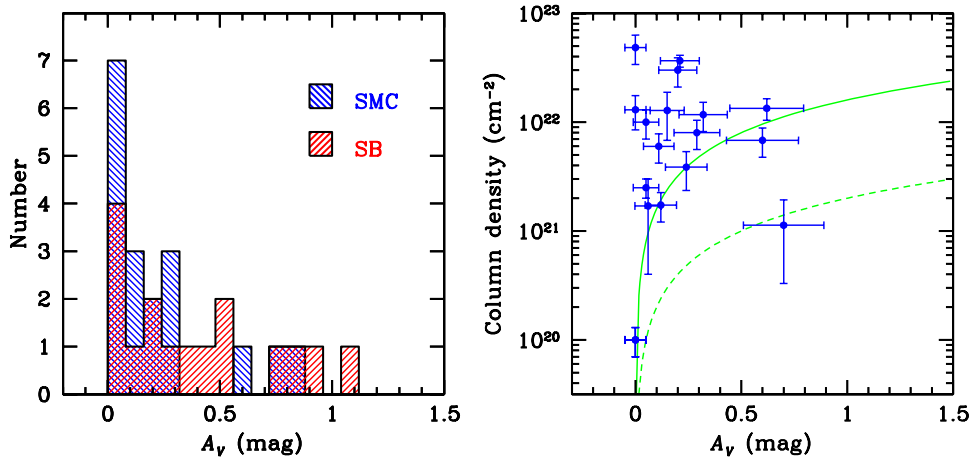


Fig. 4. – Left: distribution of the rest-frame A_V measured for our sample, assuming an SMC or starburst (SB) extinction curve. Right: comparison of the rest-frame A_V and N_{H} (assuming an SMC extinction curve). The solid line shows the SMC dust-to-gas ratio, and the dashed line shows the same ratio when normalized to solar metallicity.

on the average a larger A_V is needed in order to obtain the same reddening. In a few cases, however, we could find no solution adopting the SB curve. Our analysis, therefore, does not support the existence of “grey” dust. In particular, our data never require a flat law $A(\lambda) \sim \text{const}$ [38]. The average A_V is consistent with pre-*Swift* values [24], indicating that also with the extended *Swift* sample we have not yet probed the space of extinguished afterglows, although sampling much earlier phases than before. We caution, however, that the bursts in our sample all have a measured redshift, so they could still suffer from some selection effect against faint (and more likely extinguished) afterglows (the analysis of the few dark bursts with redshift is underway).

The right panel of fig. 4 shows a comparison between the rest-frame A_V (using the SMC extinction curve) and the hydrogen column densities N_{H} as measured from the X-ray spectra (assuming solar abundances). The (logarithmic) average is $N_{\text{H}}/A_V = 3 \times 10^{22} \text{ cm}^{-2} \text{ mag}^{-1}$, with a scatter of 0.55 dex. The solid line represents the dust-to-gas ratio as measured in the SMC. Taken at face value, the column densities are on the average larger than expected from this relation [21, 22]. We note also that our N_{H} values have been computed assuming Solar metallicity, while the SMC has a lower value ($\approx Z_{\odot}/8$). The dashed line shows the relation expected after normalizing the dust-to-gas ratio to solar metallicity, further exacerbating the discrepancy. Thus, the ISM medium in GRB host galaxies is different than that of the SMC. Several explanations have been proposed to explain the low dust content along GRB sight lines, including dust destruction [39–41] due to the intense UV flux (either from the GRB or from the neighbouring hot stars), or the young age of the stellar populations (no time enough for dust formation) [42, 43]. Alternatively, it is possible that the dust optical properties are significantly different from the local templates. Some suggestions in this direction have come from the analysis of optical absorption lines [44], even if our study does not favor flat extinction curves. It could also be that these dust grains are smaller.

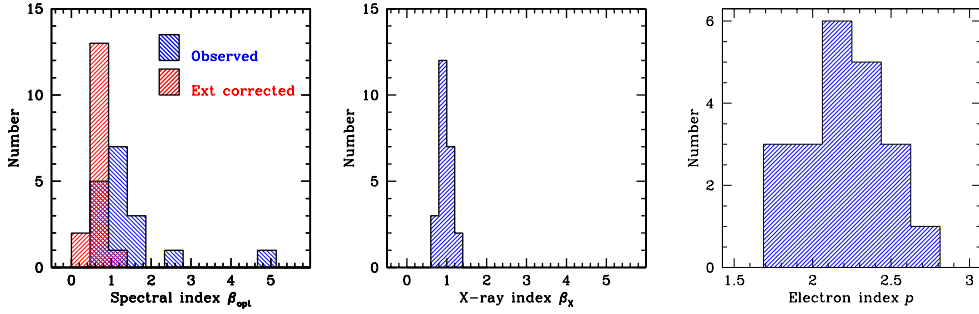


Fig. 5. – Left and middle panels: distributions of the optical and X-ray spectral indices. Right panel: distribution of the electron power law index.

3.2. GRB physics. – The first, interesting result is that the synchrotron spectrum fits remarkably well. In the analyzed sample, only one case (GRB 050904) could not be modeled with a single synchrotron spectrum. In particular, there is no need to introduce an inverse Compton component (which is anyway expected to contribute only at later times, see [45]). Thus, in contrast to the complexity in the temporal domain, a simple spectral model works well for most afterglows. Figure 5 shows the distribution of the spectral indices in the optical and X-ray ranges, as well as the inferred electron distribution power law index p . The observed optical slopes span a broad range, but after dust correction they cluster around the typical value $\beta_{opt} \approx 0.7$, with a dispersion similar to that in the X rays. The electron index p (computed as $p = 2\beta$ or $p = 2\beta + 1$ according to the location of the cooling frequency) is also clustered around its “canonical” value: $\langle p \rangle = 2.2 \pm 0.3$. Only 4/22 bursts have $p < 2$.

With the temporal and spectral decay indices, we could then check the closure relations. Of the 23 analyzed cases, 6 are fitted by an ISM model (and not by a wind), while 3 are fitted by a wind (and not by a ISM); for 13 the available data are consistent with both solutions, while for 1 no case works. For 5 bursts energy injection (or any other suitable mechanism) was required to explain a flat phase in the X-ray light curve. For a few bursts, the SED shows the cooling frequency to be close to or inside the XRT range ($\nu_c \approx 0.1\text{--}0.5$ keV). This suggests the possibility to test afterglow models by measuring the time dependence (if any) of ν_c (see also [46]).

There is another interesting feature evidenced by our SEDs. Both during the X-ray flares and during the initial steep decay phases, the optical-to-X-ray spectral index β_{OX} can be extremely hard (see the early SEDs of GRB 050319 and XRF 050416A in figs. 2 and 3). This is a confirmation also from the spectral point of view that the X-ray radiation is not (or not only) afterglow emission during these phases, but is likely of internal origin, as already suggested on the basis of temporal properties (for a recent discussion on this subject see also [47]). In this case, care must be used when determining the optical “darkness” of a GRB, since the standard β_{OX} criterium [48] may in this case be easily violated even for low-redshift, unextinguished afterglows.

* * *

This work was supported by ASI grant I/R/039/04 and MIUR grant 2005025417. DM acknowledges support from the Instrument Center for Danish Astrophysics.

REFERENCES

- [1] GALAMA T. J., VREESWIJK P. M., VAN PARADIJS J. *et al.*, *Nature*, **395** (1998) 670.
- [2] STANEK K. Z., MATHESON T., GARNAVICH P. M. *et al.*, *Astrophys. J.*, **591** (2003) L17.
- [3] HJORTH J., SOLLERMAN J., MØLLER P. *et al.*, *Nature*, **423** (2003) 847.
- [4] MALESANI D., TAGLIAFERRI G., CHINCARINI G. *et al.*, *Astrophys. J.*, **609** (2004) L5.
- [5] CAMPANA S., MANGANO V., BLUSTIN A. J. *et al.*, *Nature*, **442** (2006) 1008.
- [6] PIAN E., MAZZALI P. A., MASETTI N. *et al.*, *Nature*, **442** (2006) 1011.
- [7] TAGLIAFERRI G., ANTONELLI L. A., CHINCARINI G. *et al.*, *Astron. Astrophys.*, **443** (2005) L1.
- [8] KAWAI N., KOSUGI G., AOKI K. *et al.*, *Nature*, **440** (2006) 184.
- [9] JAKOBSSON P., LEVAN A., FYNBO J. P. U. *et al.*, *Astron. Astrophys.*, **447** (2006) 897.
- [10] MÉSZÁROS P. and REES M. J., *Astrophys. J.*, **476** (1997) 232.
- [11] ZHANG B., FAN Y.-Z., DYKS J. *et al.*, *Astrophys. J.*, **642** (2006) 354.
- [12] PANAITESCU A., MÉSZÁROS P., GEHRELS N. *et al.*, *Mon. Not. R. Astron. Soc.*, **336** (2006) 1357.
- [13] GRANOT J., KONIGL A. and PIRAN T., *Mon. Not. R. Astron. Soc.*, **370** (2006) 1946.
- [14] SARI R., PIRAN T. and NARAYAN R., *Astrophys. J.*, **497** (1998) L17.
- [15] VREESWIJK P. M., ELLISON S. L., LEDOUX C. *et al.*, *Astron. Astrophys.*, **419** (2004) 927.
- [16] CAMPANA S., ROMANO P., COVINO S. *et al.*, *Astron. Astrophys.*, **449** (2006) 61.
- [17] BERGER E., PENPRASE B. E., CENKO S. B. *et al.*, *Astrophys. J.*, **642** (2006) 979.
- [18] PROCHASKA J. X., BLOOM J. S., CHEN H.-W. *et al.*, *Astrophys. J.*, **611** (2004) 200.
- [19] WIERSEMA K., SAVAGLIO S., VREESWIJK P. M. *et al.*, *Astron. Astrophys.*, **464** (2007) 529.
- [20] FYNBO J. P. U., GOROSABEL J., DALL T. H. *et al.*, *Astron. Astrophys.*, **373** (2001) 796.
- [21] GALAMA T. J. and WIJERS R. A. M. J., *Astrophys. J.*, **549** (2001) L209.
- [22] STRATTA G., FIORE F., ANTONELLI L. A. *et al.*, *Astrophys. J.*, **608** (2004) 846.
- [23] NARDINI M., GHISELLINI G., GHIRLANDA G. *et al.*, *Astron. Astrophys.*, **451** (2006) 821.
- [24] KANN D. A., KLOSE S. and ZEH A., *Astrophys. J.*, **641** (2006) 993.
- [25] STARLING R. L. C., WIJERS R. A. M. J., WIERSEMA K. *et al.*, to be published in *Astrophys. J.*, astro-ph/0610899.
- [26] CHINCARINI G., MANGANO V., MORETTI A. *et al.*, astro-ph/0511107 (2005).
- [27] NOUSEK J. A., KOUVELIOTOU C., GRUPE D. *et al.*, *Astrophys. J.*, **642** (2006) 389.
- [28] CHINCARINI G., MORETTI A., ROMANO P. *et al.*, these proceedings.
- [29] PEI Y. C., *Astrophys. J.*, **395** (1992) 130.
- [30] CALZETTI D., ARMUS L., BOHLIN R. C. *et al.*, *Astrophys. J.*, **533** (2000) 682.
- [31] CUSUMANO G., MANGANO V., ANGELINI L. *et al.*, *Astrophys. J.*, **639** (2006) 316.
- [32] WOŹNIAK P. R., VESTRAND W. T., WREN J. A. *et al.*, *Astrophys. J.*, **627** (2005) L13.
- [33] MASON K., BLUSTIN A., BOYD P. *et al.*, *Astrophys. J.*, **639** (2006) 311.
- [34] QUIMBY E., RYKOFF E., YOST S. *et al.*, *Astrophys. J.*, **640** (2006) 402.
- [35] MANGANO V., CUSUMANO G., LA PAROLA V. *et al.*, *Astrophys. J.*, **654** (2007) 403.
- [36] HOLLAND S. T., BOYD P. T., GOROSABEL J. *et al.*, *Astron. J.*, **133** (2006) 122.
- [37] SODERBERG A. M., NAKAR E., CENKO S. B. *et al.*, to be published in *Astrophys. J.*, astro-ph/0607511.
- [38] MAIOLINO R., MARCONI A. and OLIVA E., *Astron. Astrophys.*, **365** (2001) 37.
- [39] GALAMA T. J. and WIJERS R. A. M. J., *Astrophys. J.*, **549** (2001) L209.
- [40] WAXMAN E. and DRAINE B. T., *Astrophys. J.*, **537** (2000) 796.
- [41] PERNA R. and LAZZATI D., *Astrophys. J.*, **580** (2002) 261.
- [42] WATSON D., FYNBO J. P. U., LEDOUX C. *et al.*, *Astrophys. J.*, **652** (2006) 1011.
- [43] CAMPANA S., LAZZATI D., RIPAMONTI E. *et al.*, *Astrophys. J.*, **654** (2007) L17.
- [44] SAVAGLIO S. and FALL S. M., *Astrophys. J.*, **614** (2004) 293.
- [45] HARRISON F. A., YOST S. A., SARI R. *et al.*, *Astrophys. J.*, **559** (2001) 123.
- [46] BUTLER N. R. and KOCEVSKI D., to be published in *Astrophys. J.*, astro-ph/0612564.
- [47] GHISELLINI G., GHIRLANDA G., NAVA L. and FIRMANI C., *Astrophys. J.*, **658** (2007) L75.
- [48] JAKOBSSON P., HJORTH K., FYNBO J. P. U. *et al.*, *Astrophys. J.*, **617** (2004) L21.